Landslide Susceptibility Zonation Using GIS-Based Frequency Ratio Approach in the Kulon Progo Mountains Area, Indonesia

Egy Erzagian, Wahyu Wilopo, and Teuku Faisal Fathani

Abstract

Landslides cause many casualties, environmental damage, property losses, and psychological impacts. Landslides frequently occur in the Kulon Progo Mountains area of Indonesia and are especially triggered by high-intensity rainfall between November and March. Research on landslide susceptibility in the Kulon Progo Mountains area can be a relevant tool to prevent or reduce the risk of landslide potential. Therefore, this research aims to develop a landslide susceptibility map using the frequency ratio (FR) method. Controlling factors, namely, elevation, slope, aspect, lithology, lineament density, distance from streams, distance from roads, land use, and rainfall, were combined with landslide data to develop a landslide susceptibility map by GIS software. Seven hundred and forty-four landslide data points were acquired from field surveys, Google Earth image interpretation, and the Regional Disaster Management Agency (BPBD) of the Kulon Progo, Purworejo, and Magelang regencies. Landslide data were randomly selected for map modeling (80%) and validation (20%). The FR analysis shows that the research area can be classified into four landslide susceptibility zones based on the LSI value: low (LSI 4.05–7.85), moderate (LSI 7.86–9.85), high (LSI 9.86–12.81), and very high (LSI 12.82–19.46). The landslide susceptibility map was validated using the area under the curve (AUC) method, resulting in a success rate of 80.1% and a predictive rate of 81.3%.

1 Introduction

The Kulon Progo Mountains form a mountainous area in the southern part of Java Island, Indonesia. Tectonic processes and volcanic activities that formed the Kulon Progo Mountains area have occurred from the Tertiary to the Quaternary (Widagdo et al. 2018a, b). The Kulon Progo Mountains are generally composed of weathered and altered volcanic rocks that form a thick layer of soil with clay minerals. This weathered rock and thick soil layer is prone to landslides (Fookes et al. 2005).

Landslides are generally controlled by several factors, such as slope, lithology, geological structure, hydrological conditions, land use, and rainfall (Skilodimou et al. 2018; Conforti and Ietto 2020; Mersha and Meten 2020). Landslide activity in the Kulon Progo Mountains increases yearly, especially the activity triggered by high-intensity rainfall, for example, the Cempaka tropical cyclone in 2017–2018. The Regional Disaster Management Agency reported 744 landslide events in the period of 2015–2020. Landslides in the Kulon Progo Mountains area have caused numerous casualties, environmental damage, property losses, and psychological impacts. Therefore, landslide susceptibility maps of the Kulon Progo Mountains provide an important tool to prevent or reduce landslide risk. In addition, landslide susceptibility maps can be used by decision-makers for land use planning, landslide prevention, monitoring, and mitigation actions.

The purpose of this research is to develop a landslide susceptibility map. This research uses data on the distribution of landslide occurrence points and factors controlling landslides, such as elevation, slope, aspect, lithology, lineament density, distance from streams, distance from roads,

E. Erzagian · W. Wilopo (✉)
Department of Geological Engineering, Universitas Gadjah Mada, Yogyakarta, Indonesia
e-mail: egyerzagian@mail.ugm.ac.id; wilopo_w@ugm.ac.id

T. F. Fathani
Department of Civil and Environmental Engineering, Universitas Gadjah Mada, Yogyakarta, Indonesia
e-mail: tfathani@ugm.ac.id

land use, and rainfall, to identify the landslide susceptibility zones.

2 Research Area

The research area is the Kulon Progo Mountains, which were geomorphologically formed as a Tertiary volcanic product (Widagdo et al. 2018a, b). This area includes two provinces: the Special Region of Yogyakarta and Central Java. It consists of 3 regencies, namely, Kulon Progo, Purworejo, and Magelang, and 12 subdistricts, which are Bagelen, Bener, Borobudur, Girimulyo, Kalibawang, Kaligesing, Kokap, Loano, Pengasih, Purworejo, Salaman, and Samigaluh (Fig. 1). The area is geographically located from 110°02′11.14"E to 110°16′02.30"E and 7°33′01.16"S to 7°52′08.02"S and covers an area of approximately 533.43 km^2.

The area has elevations between 19 and 976 masl. The morphology comprises a steeply sloping area with a height of up to 976 masl, a moderately sloping area with a lower elevation, and a gently sloping area with a low elevation. In the area, streams have flow directions of NW–SE on the west slope, SE–NW on the east slope, SW–NE on the north slope, and NE–SW on the south slope. The area is regionally composed of Tertiary–Quaternary volcanic and intrusive rocks, especially the Kebo-Butak Formation and andesite intrusion. The stratigraphy of the Kulon Progo Mountains area from oldest to youngest (Rahardjo et al. 1995) is as follows:

1. The Nanggulan Formation (Teon), the oldest rock formation, consists of sandstones with intercalations of lignite, sandy marl, claystone with limonite concretions, intercalations of marl and limestone, sandstone, and tuff. The formation age is Eocene–Oligocene.
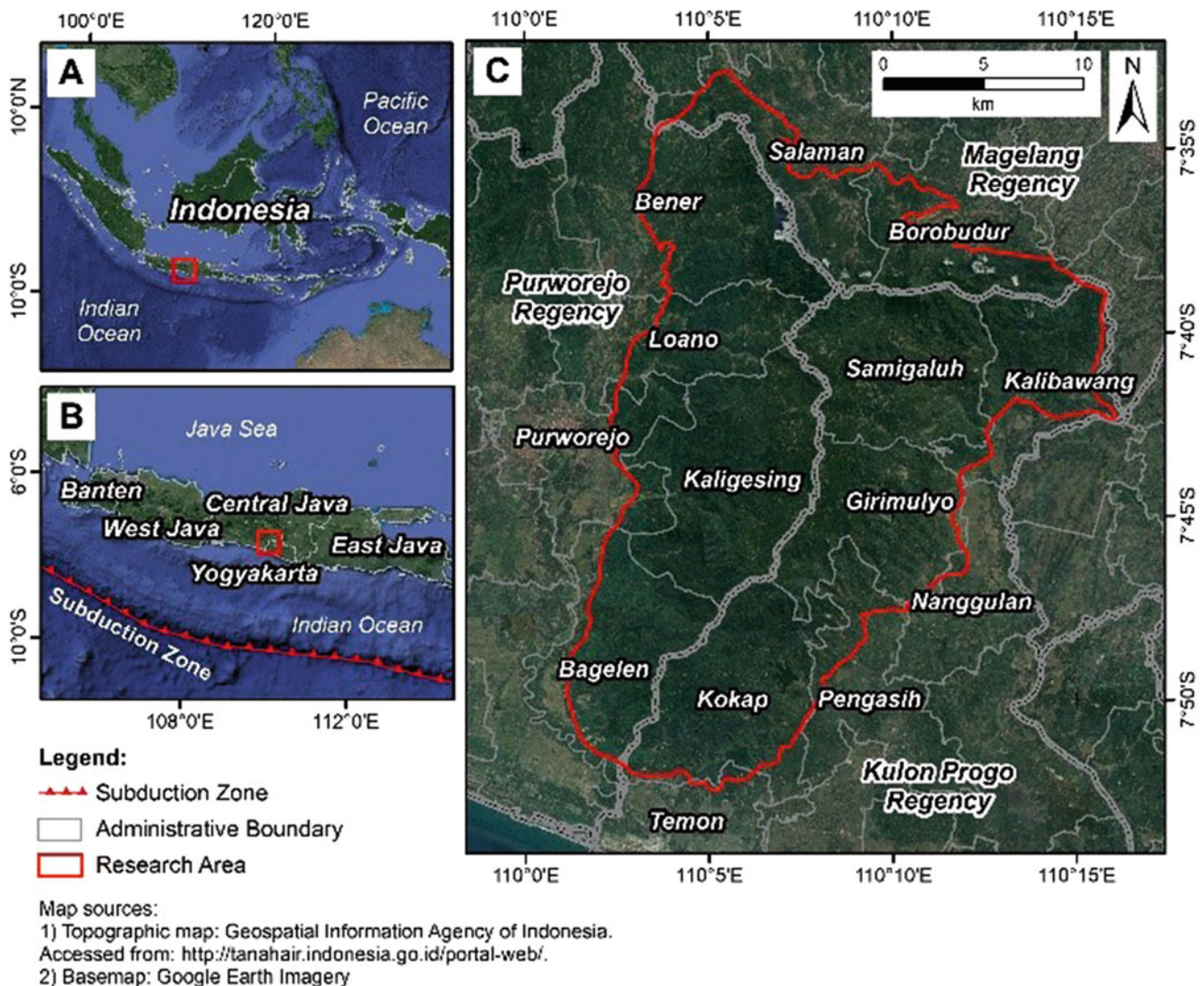

Fig. 1 (**a**) Map of Indonesia; (**b**) map of Java Island; and (**c**) research area

2. The Kebo-Butak Formation (Tmok) is unconformably deposited above the Nanggulan Formation. This formation consists of andesitic breccia, tuff, lapilli tuff, agglomerates, and intercalations of andesitic lava flows. The formation age is Oligocene–Miocene.
3. Intrusive rocks break through to the bottom of the Kebo-Butak Formation. The intrusive rocks consist of an andesite intrusion (a) and a dacite intrusion (da). The rock age is Miocene.
4. The Jonggrangan Formation (Tmj) is unconformably deposited above the Kebo-Butak Formation. This formation is exposed in the middle of the Kulon Progo Mountains. It consists of conglomerate, tuffaceous marl, carbonate sandstone, and claystone with lignite at the bottom, while layered limestone and coral limestone make up the top. The formation age is early Miocene–middle Miocene.
5. The Sentolo Formation (Tmps) is conformally deposited and has an interfingering contact with the Jonggrangan Formation. This formation consists of limestone and marl sandstone. The formation age is middle Miocene–Pliocene.
6. Young volcanic deposits of Merapi Volcano (Qmi) are unconformably deposited above the Sentolo Formation. This formation comprises undifferentiated tuff, ash, breccia, agglomerate, and lava flows. The formation age is the Pleistocene.
7. The alluvium and colluvium (Qa) consist of gravel, sand, silt, and clay along large rivers and coastal plains. The colluvium (Qc) consists of unsorted debris from the Kebo-Butak Formation.

3 Methodology

Landslides may reoccur under similar circumstances as previous landslides, so it is necessary to identify potential landslides by determining the factors that control them (Lee and Talib 2005). The analysis of the landslide susceptibility map is carried out using the frequency ratio (FR) method and the overlay process using GIS. The FR method is one of the statistical methods used in mapping landslide susceptibility using two variables (Mersha and Meten 2020). In this study, 80% of landslide occurrence points are used to analyze landslide susceptibility maps, while 20% are used for validation.

The landslide susceptibility map used in the frequency ratio method is based on the relationship between the landslide distribution and each controlling factor. The landslide-controlling factors in this study are elevation, slope, aspect, lithology, lineament density, distance from streams, distance from roads, land use, and rainfall. Each landslide-controlling factor is classified into several categories and then integrated with the distribution of landslide occurrence points. The FR for each category is obtained through statistical calculations, as shown in Eq. 1 (Tazik et al. 2014).

The FR map for each landslide-controlling factor is processed using GIS tools by setting the FR value. The calculated FR value shows the correlation degree between landslides and certain factor classes (Rasyid et al. 2016; Mersha and Meten 2020). An FR value equal to 1 is the average value for the occurrence of movement for a specific factor. FR > 1 indicates a high potential for landslides, while FR < 1 indicates a low potential.

$$FR = \frac{\frac{D_i}{A_i}}{\frac{\sum_{i=1}^{N} D_i}{\sum_{i=1}^{N} A_i}} \tag{1}$$

where.

FR: *Frequency ratio* of each class for a certain factor (i)
D_i: Number of landslide points for a certain factor (i)
A_i: Area of a class for a certain factor (i)
N: Number of factors

The overlay process combines several maps of landslide-controlling factors. All the FR values on each controlling factor map are summed to derive the landslide susceptibility index (LSI) value, as shown in Eq. 2 (Tazik et al. 2014).

$$LSI = FR_1 + FR_2 + FR_3 + \ldots + FR_N \tag{2}$$

Using the Jenks natural breaks method, the landslide susceptibility map is classified based on the LSI value. The Jenks natural breaks method produces a map that can be interpreted by showing the spatial probability of future landslides ranging from very low to very high landslide susceptibility (Aditian et al. 2018).

The landslide susceptibility map validation is carried out using the area under the curve (AUC) method by making both success and predictive rate curves (Lee and Talib 2005; Mersha and Meten 2020). The success rate on the AUC indicates the accuracy and quality of the resulting map developed based on modeling data, while the AUC prediction rate explains the capacity of the suggested map to predict the landslide susceptibility (Yalcin and Bulut 2007).

4 Dataset and Analysis

The collected data in this study consist of the distribution of landslide events and controlling factors processed using GIS. Nine landslide factors, including elevation, slope, aspect,

Table 1 Research dataset

Data	Data Source	Usage
Digital elevation model (DEM)	DEMNAS with 8.23 m × 8.23 m grid resolution (Geospatial Information Agency of Indonesia 2023)	Elevation, slope, aspect, stream, lineament
Geological map	Geological map of the Yogyakarta Sheet, Java, the scale of 1:100,000 (Rahardjo et al. 1995)	Lithology and lineament
Geological structure map	Lineament's interpretation and geological structure maps of the Kulon Progo mountains area (Rahardjo et al. 1995; Widagdo et al. 2018a, b)	Lineament
Road distribution	Road map scale of 1:25,000 (Geospatial Information Agency of Indonesia (2015–2019))	Road
Land use map	Land use map scale of 1:25,000 (Geospatial Information Agency of Indonesia (2015–2019))	Land use
Rainfall data	Rainfall data reported in the 2011–2020 period for each regency (Central Bureau of Statistics of Kulon Progo 2021; Central Bureau of Statistics of Purworejo 2021; Central Bureau of Statistics of Magelang 2021)	Rainfall
Landslide database	Rotational landslide event summary data from each regency (regional disaster management agency)	Landslide events
Satellite imagery	Google earth satellite imagery	Landslide events

lithology, lineament density, distance from streams, distance from roads, land use, and rainfall, are used in this research. Table 1 shows the data sources used to analyze landslide susceptibility maps.

Landslide events are verified and added via Google Earth satellite image interpretation (Fig. 2). Rotational and translational slides are the dominant types of landslides. The number of landslides in the research area is 744 points, where 595 points (80% of the total landslide events) are used as modeling data to prepare landslide susceptibility maps and 149 points (20% of the total landslide events) are used to validate the landslide susceptibility map. Landslide events for modeling and validation are randomly selected.

An elevation, a part of morphology, is formed by a combination of tectonic activity, erosion-weathering processes, and climatic effects (Ilia and Tsangaratos 2016). Elevations contribute indirectly to landslide events. The elevation map (Fig. 3a) was generated from DEM analysis and divided into five classes, i.e., 0–200 masl, 201–400 masl, 401–600 masl, 601–800 masl, and 801–1000 masl.

An aspect indicates the slope's direction and affects the slope's exposure to sunlight, wind direction, degree of saturation, and discontinuity conditions (Psomiadis et al. 2020; Mersha and Meten 2020). The aspect map (Fig. 3b) is generated from DEM data and divided into ten classes, i.e., flat (−1), north (0–22.5), northeast (22.5–67.5), east (67.5–112.5), southeast (112.5–157.5), south (157.5–202.5), southwest (202.5–247.5), west (247.5–292.5), northwest (292.5–337.5), and north (337.5–360).

A slope, as a geomorphological component, significantly contributes to landslides. The potential increases due to the greater driving force on steep slope conditions. The slope data are obtained from digital elevation model (DEM) analysis with an 8.23 × 8.23 m grid resolution. The slope map from the DEM analysis is divided into four slope categories, i.e., 0°–15°, 16°–25°, 26°–35°, and 36°–57°, as shown in Fig. 3c.

Landslides commonly occur on slopes composed of weathered rock and residual soil with a thick layer and contain clay minerals (Fookes et al. 2005). Lithological data are obtained from the Geological Map of the Yogyakarta Sheet (Rahardjo et al. 1995). The lithologic map is divided into seven units based on rock formations, i.e., the Nanggulan Formation, Kebo-Butak Formation, intrusive rocks, Jonggrangan Formation, Sentolo Formation, young volcanic deposits of Merapi, and alluvium–colluvium deposits, as shown in Fig. 3d. The field survey shows that almost all the rocks are weathered and intrusive rocks. This is probably due to the dense geological structures that speed up the weathering process.

Lineaments generally indicate fractures, discontinuities, and shear zones that can contribute to landslides (Sarkar and Kanungo 2004). The lineament data are obtained from digital elevation model (DEM) analysis by considering secondary data, including geological maps developed by previous researchers, lineament interpretation, and geological structure maps. The lineament density is analyzed using the kernel density function in GIS. The lineament density map of the geological structure is classified into four categories, i.e., 0.31–1.45 km/km², 1.46–2.05 km/km², 2.06–2.55 km/km², and 2.56–3.58 km/km² (Fig. 3e).

The distance from streams is one of the factors that can indicate landslides and associated erosion processes to describe slope changes. The distance from streams is generated using the buffering function in GIS analysis. Stream data are obtained from watershed analysis using a DEM with a 200 × 200 m threshold and verified by the 1:25,000 scale topographic map. The distance from streams map (Fig. 3f) is categorized into four categories, i.e., <100 meters, 100–200 meters, 200–400 meters, and > 400 meters.

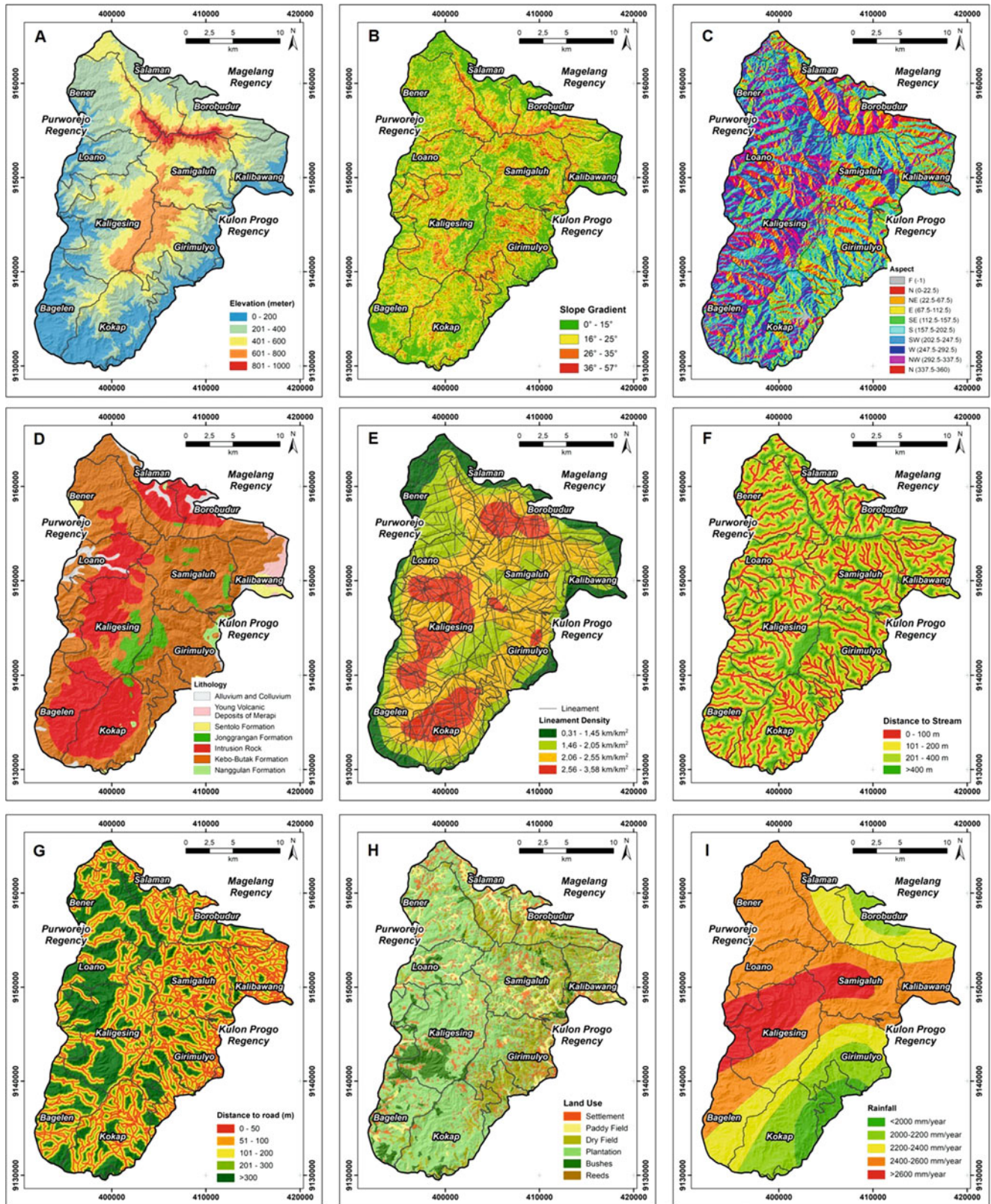**Fig. 2** (**a**) Landslide event distribution map; (**b**) verification based on Google Earth image interpretation
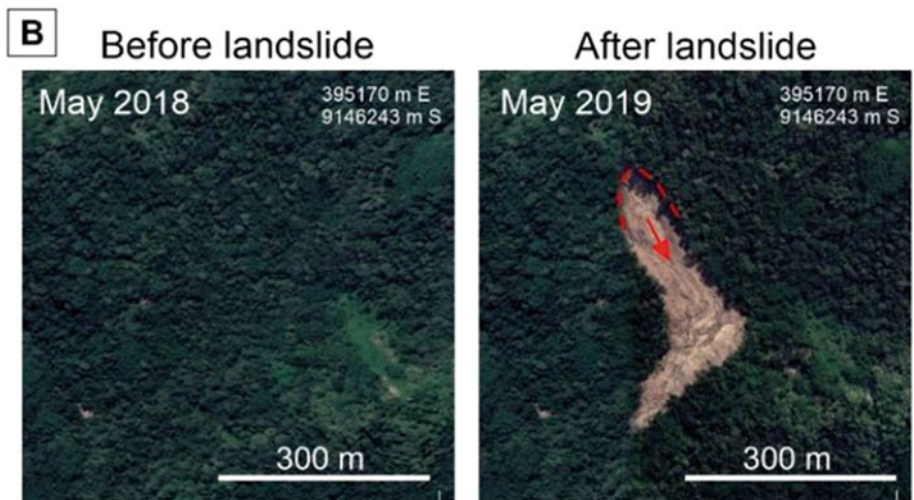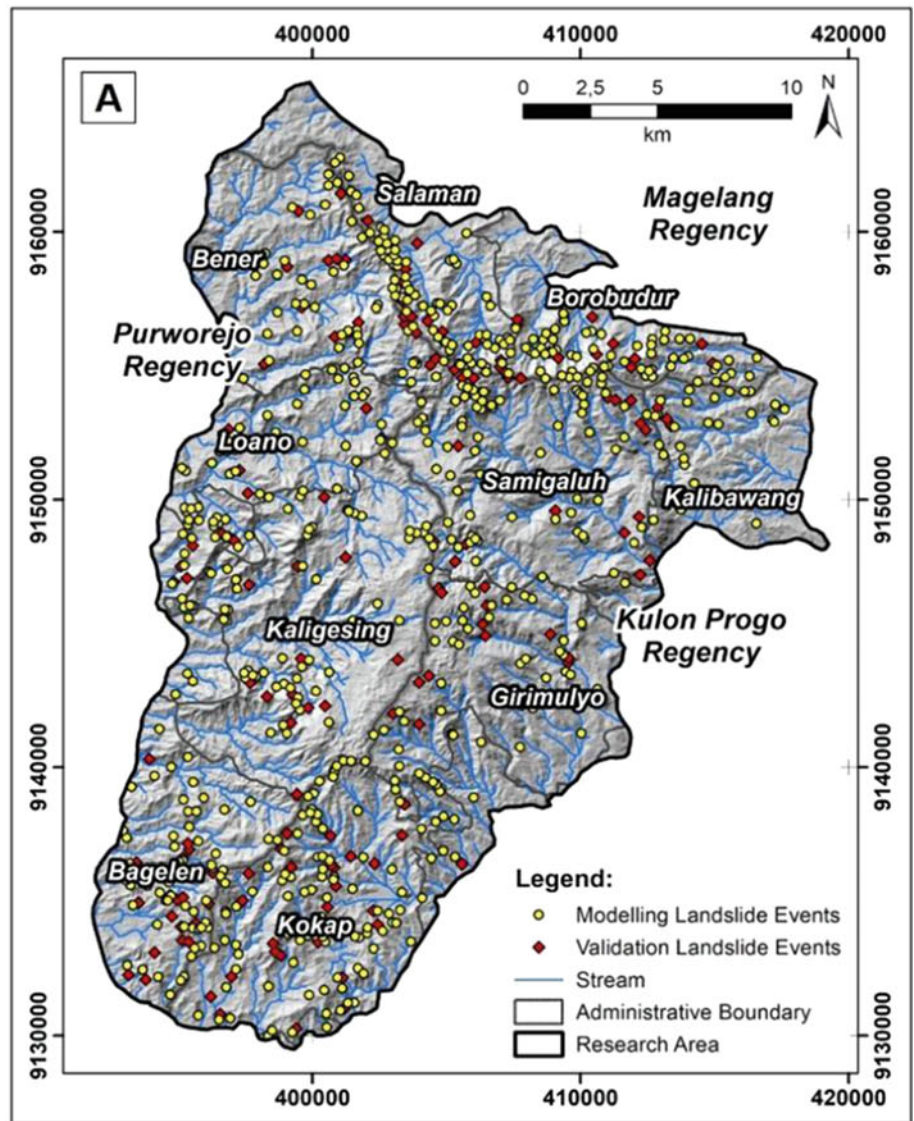
Fig. 3 Landslide-controlling factor maps: (**a**) elevation; (**b**) slope; (**c**) aspect; (**d**) lithology; (**e**) lineament density; (**f**) distance from streams; (**g**) distance from roads; (**h**) land use, and (**i**) rainfall

Road construction is closely related to vegetation removal and excavation, which can form steep slopes (Psomiadis et al. 2020). The road network in the study area, which consists of main roads and local roads, is one of the factors that can affect landslides. The road distance map (Fig. 3g) was developed from the buffer zone of the road network without including footpaths and divided into five classes, namely 0–50 m, 51–100 m, 101–200 m, 201–300 m, and > 300 m.

Land use has significant control over erosion and deposition. Land use, such as vegetation or plant residues, can withstand raindrops, increase infiltration, reduce runoff velocity, and increase water flow capacity (Akgün and Türk 2011). Land use with sparse vegetation generally shows faster erosion and slope conditions prone to landslides (Yalcin and Bulut 2007). The land use map (Fig. 3h) is classified into six land use types, i.e., settlements, paddy fields, dry fields, plantations, bushes, and reeds. Land use types are digitized from the 1:25,000 scale topographic map.

Rainfall intensity is one of the major triggers for landslides that can directly impact settlements (Haque et al. 2019). Prolonged and high-intensity rainfall generally triggers landslides because it can increase hydrostatic and pore water pressure below the surface. Rainfall data are obtained from rainfall data reports from the Kulon Progo, Purworejo, and Magelang regencies in the 2011–2020 period. Landslide occurrence distribution data are obtained from the Regional Disaster Management Agency (BPBD) of each regency. The rainfall data that were used have a longer period than the available landslide data. More accurate results can be obtained with a longer period of hydrological data. The annual rainfall intensity data for 10 years (2010–2019) are obtained from 12 nearby rainfall stations. The annual rainfall average value is 2409 mm/year, with a range of data of 1786–3021 mm/year. The rainfall map is analyzed using GIS interpolation with the kriging method based on the average annual rainfall data of each station. The rainfall map (Fig. 3i) is divided into five categories, i.e., <2000 mm/year, 2000–2200 mm/year, 2200–2400 mm/year, 2400–2600 mm/year, and > 2600 mm/year.

5 Result & Discussion

The results of the FR calculation show that the landslide susceptibility level is higher as the degree of the slope increases. The landslide-controlling factor, with FR > 1, mainly shows a high frequency of landslides, while FR <1 shows a lower frequency. The 801–1000 masl elevation has the highest FR value, significantly influencing landslide events, while the lowest FR value is the 0–200 masl elevation. The slope with angles of >15° has a significant contribution to landslides. The highest FR value for the slope factor is the slope with angles of 36°-57°, while the lowest is in the slope with angles of 0°-15°. In terms of aspect, the FR value of the north class (0–22.5) has the highest FR value, followed by north (337.5–360) and northeast (22.5–67.5). The lowest FR value for aspect is the flat category (−1).

In terms of lithology, Kebo-Butak Formation causes significant landslides in the research area, followed by intrusive rocks (andesite and dacite), the Jonggrangan Formation, and Nanggulan Formation. Kebo-Butak Formation generally undergoes weathering and alteration to form a thick layer of soil and is prone to landslides. A low number of landslide occurrences is found in alluvium deposits, colluvium deposits, the young volcanic deposits of Merapi Volcano, and the Sentolo Formation. The lineament density of 2.56–3.58 km/km^2 has the highest FR value and greatly contributes to landslides. A lineament is a weak plane that can indicate geological structures (such as joints and faults) or cracks, accelerate the weathering process, and allow water to infiltrate the slope. In general, the number of landslides increases as the lineament density increases. For the distance from streams, a distance from the river of >400 m significantly contributes to landslides, while a distance from the river of <100 m has a minor contribution. This result shows that the stream does not significantly control landslide occurrences.

For land use, frequent landslides are usually influenced by reeds, bushes, and dry fields. Areas with reeds, bushes, and dry fields usually have sparse vegetation, and consequently, erosion occurs more quickly, and the areas are thus prone to landslides. The results of the FR calculation show that the frequency of landslides increases as the intensity of rainfall increases. A rainfall of 2200–2400 mm/year significantly contributes to landslides.

The LSI values are arranged as LSI maps and classified into ten categories to determine the FR validation. The FR values for each landslide-controlling factor are summed and overlaid in GIS processing to produce the LSI value. The LSI value calculated through this analysis can describe the level of landslide susceptibility. The LSI value has a range of 4.05–19.46.

Using the Jenks natural breaks method, the reclassification of LSI values produces four landslide susceptibility zones. This method is a standard method that is commonly used and has a high level of reliability (North 2009). The four landslide susceptibility zones in the research area are low (LSI 4.05–7.85), moderate (LSI 7.86–9.85), high (LSI 9.86–12.81), and very high (LSI 12.82–19.46).

(a) The low landslide susceptibility zone (LSI 4.05–7.85) has an area of approximately 172.51 km^2 (32,34% of the total area). This zone is on a plain and sloping area adjacent to the Kulon Progo Mountains. The total number of landslides in this zone is 28 points; therefore, the landslide density is 0.162 per km^2.

Fig. 4 Landslide susceptibility map of the research area
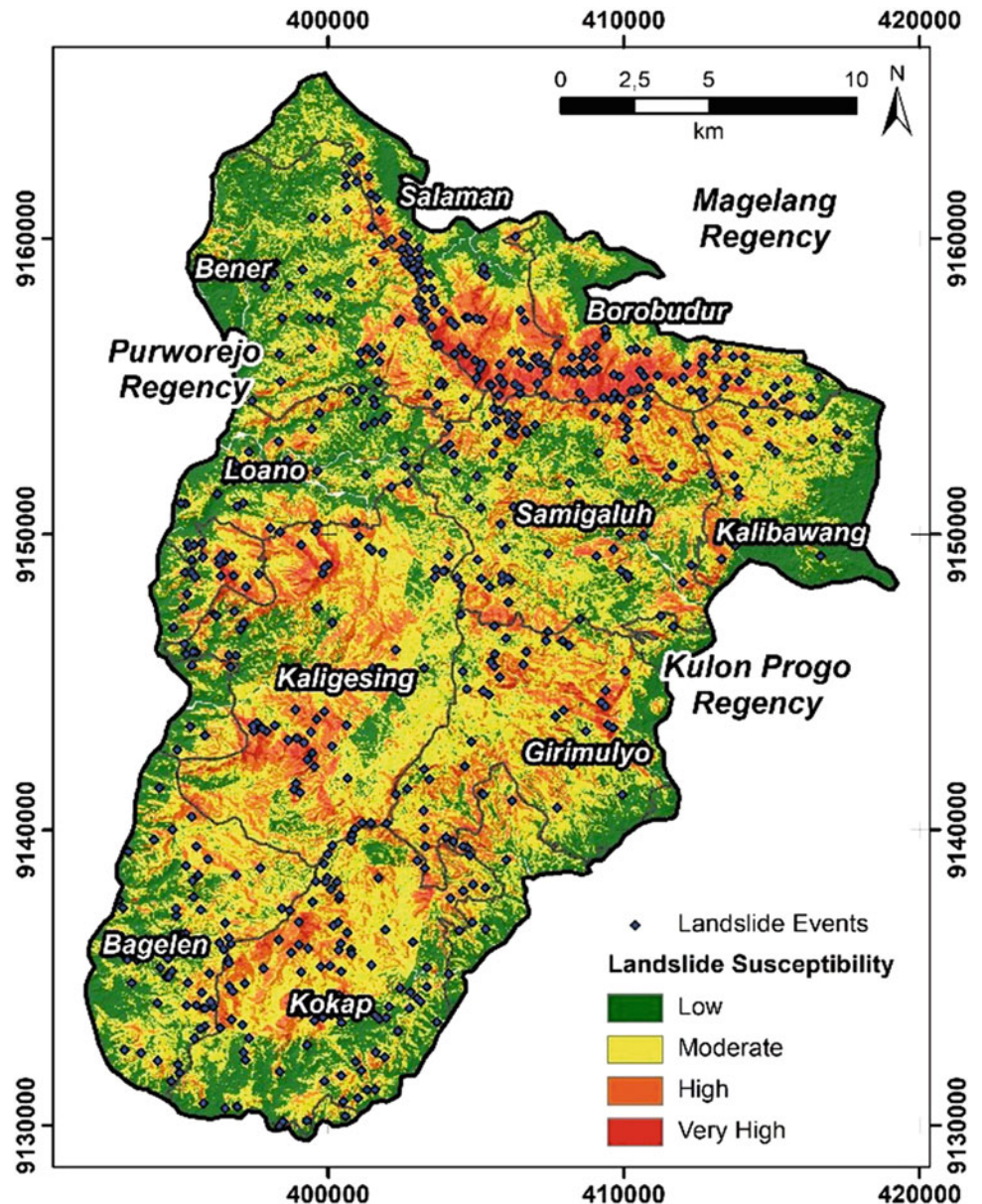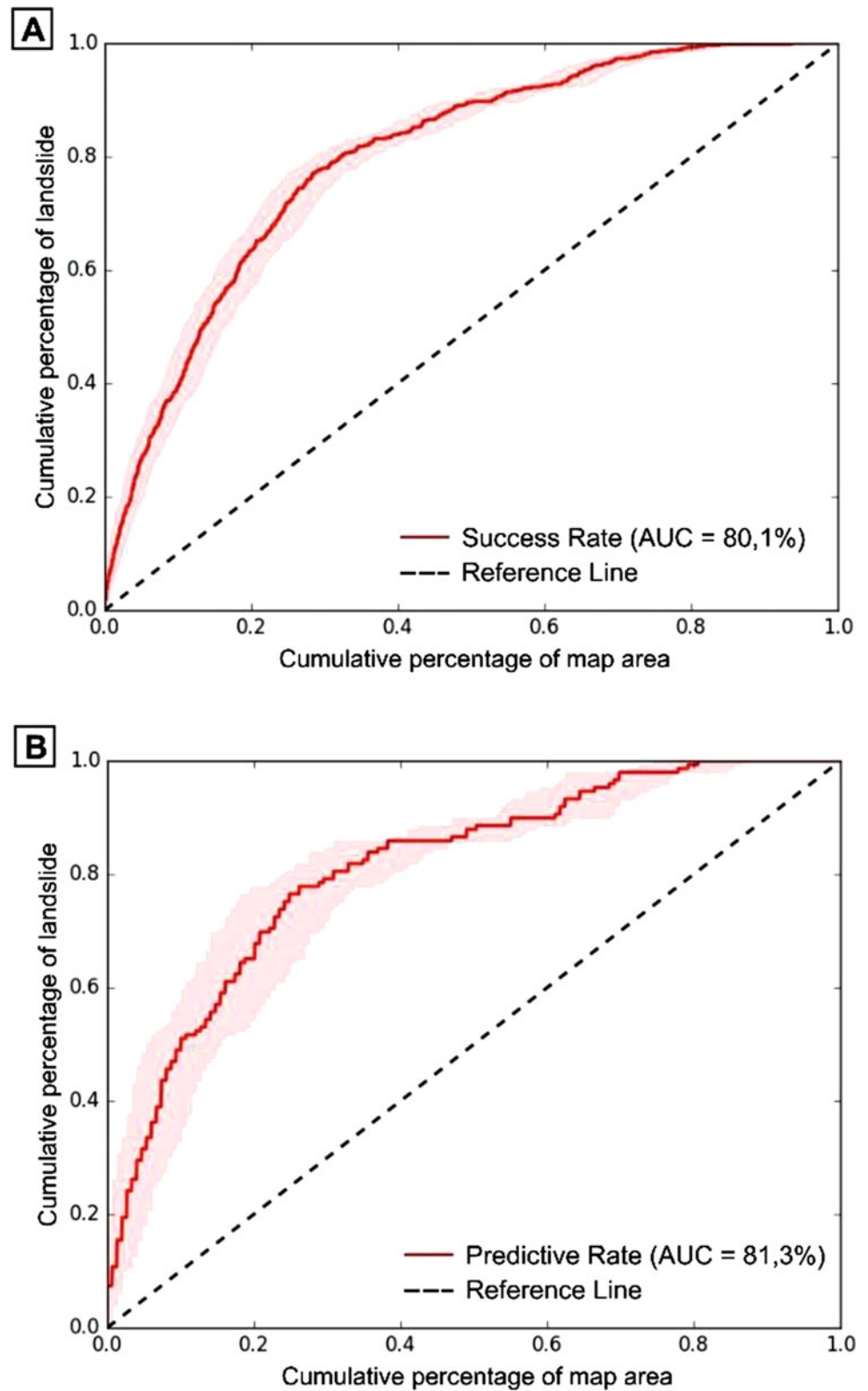

(b) The moderate landslide susceptibility zone (*LSI* 7.86–9.85) has an area of 219.39 km² (41.13% of the total area). The total number of landslides in this zone is 163 points. The landslide density in this zone is 0.742 per km². In general, an intermediate landslide susceptibility zone can be found in almost all areas of the Kulon Progo Mountains, especially in the Girimulyo, Kokap, Loano, and Bagelen areas.

(c) The high landslide susceptibility zone (*LSI* 9.86–12.81) has an area of 118.94 km² (22.30% of the total area). This zone can be found in almost all areas of the Kulon Progo Mountains and is mainly concentrated in the Kokap, Kaligesing, Samigaluh, Kalibawang, Salaman, and Borobudur subdistricts. The total number of landslides in these areas is the highest, with 396 landslides, resulting in a density of 3.32 per km².

The very high landslide susceptibility zone (*LSI* 12.82–19.46) has an area of 22.59 km² (4.23% of the total area). The total number of landslides in this zone is 207, with a density of 6.90 per km². Most of the hills with steep slopes comprise this zone, mainly concentrated in Samigaluh, Bener, Salaman, and Borobudur subdistricts (Fig. 4 and Table 2).

Elevation, slope, aspect, lineament density, and rainfall significantly contribute to the high and very high susceptibility zones. In addition, the high and very high susceptibility zones are also located mainly in weathered intrusive rocks and bushes. Most of the landslides occurred in the high susceptibility zone; however, the densest landslides occurred in the very high-susceptibility zone. The AUC method was used to validate the success and prediction rates of the landslide susceptibility map. Figure 5 shows the graphic of the

Table 2 Classes and the FR calculation for each landslide-controlling factor

Factor	Class	A_i (km^2)	$\sum A_i$ (km^2)	D_i	$\sum D_i$	FR
Elevation	0–200 masl	120.11	533.43	89	595	0.66
	201–400 masl	212.14		211		0.89
	401–600 masl	123.62		174		1.26
	601–800 masl	68.45		121		1.58
	801–1000 masl	9.11		38		3.74
Slope	0°-15°	213.9	533.43	0	595	0.00
	16°-25°	217.32		210		0.87
	26°-35°	93.41		314		3.01
	36°-57°	9.07		71		7.02
Aspect	F (−1)	11.48	533.43	4	595	0.31
	N (0–22.5)	30.85		70		2.03
	NE (22.5–67.5)	65.74		106		1.45
	E (67.5–112.5)	60.18		89		1.33
	SE (112.5–157.5)	64.63		63		0.87
	S (157.5–202.5)	75.51		62		0.74
	SW (202.5–247.5)	74.69		57		0.68
	W (247.5–292.5)	60.98		43		0.63
	NW (292.5–337.5)	60.81		50		0.74
	N (337.5–360)	28.56		51		1.60
Lithology	Alluvium and colluvium	19.72	533.43	5	595	0.23
	Young volcanic deposits of Merapi	7.84		1		0.11
	Sentolo formation	9.66		1		0.09
	Jonggrangan formation	25.30		20		0.71
	Intrusive rocks	155.11		177		1.02
	Kebo-Butak formation	311.88		390		1.12
	Nanggulan formation	3.92		1		0.23
Lineament density	0.31–1.45 km/km^2	65.18	533.43	28	595	0.39
	1.46–2.05 km/km^2	152.4		126		0.74
	2.06–2.55 km/km^2	219.01		187		0.77
	2.56–3.58 km/km^2	96.84		255		2.36
Distance from streams	<100 meter	129.38	533.43	110	595	0.76
	100–200 meter	120.86		127		0.94
	200–400 meter	188.35		212		1.01
	>400 meter	94.84		146		1.38
Distance from roads	0–50 meter	108.29	533.43	129	595	1.07
	51–100 meter	84.6		73		0.77
	101–200 meter	117.9		104		0.79
	201–300 meter	71.24		76		0.96
	>300 meter	151.4		130		0.77
Land use	Settlements	54.34	533.43	26	595	0.43
	Paddy fields	36.83		12		0.29
	Dry fields	91.93		167		1.63
	Plantations	311.41		321		0.92
	Bushes	37.64		67		1.60
	Reeds	1.28		3		2.10
Rainfall	<2000 mm/year	27.53	533.43	24	595	0.78
	2000–2200 mm/year	75.69		79		0.94
	2200–2400 mm/year	118.04		182		1.38
	2400–2600 mm/year	234.35		242		0.93
	>2600 mm/year	77.82		68		0.78

Fig. 5 (**a**) Success rate and (**b**) predictive rate curve for landslide susceptibility map validation

success and predictive rate curves, with the cumulative percentage of landslides on the x-axis and the cumulative percentage of map area on the y-axis. The validation value of the landslide susceptibility map is obtained from the calculation of the area under the curve. As a result, the success rate of the landslide susceptibility map is 80.1%, and the prediction rate is 81.30%. The validation values show very good results. This result is better than the previous research (Erzagian

et al. 2023), which only had a success rate of 76.62% and a prediction rate of 75.34% using six controlling factor parameters. Development of landslide susceptibility map using more parameters will increase the accuracy of the map.

6 Conclusion

Landslide susceptibility mapping using the FR method in the Kulon Progo Mountains area, Indonesia, resulted in four landslide susceptibility zones, i.e., low, moderate, high, and very high. A high elevation, north-facing aspect, steep slope, high lineament density, and high rainfall intensity significantly control the high-susceptibility zones. More than half of the study area has high- and very high-susceptibility zones in the weathered intrusive rock unit and bushes. Very high landslide susceptibility zones can be found in the Kaligesing, Girimulyo, Samigaluh, Kalibawang, Bener, Salaman, and Borobudur subdistricts. The landslide susceptibility map developed with the FR method has a success rate of 80.1% and a prediction rate of 81.30%, which can be categorized as a good result. The landslide susceptibility map can be used as basic information for land use planning and mitigation by the local government.

References

Aditian A, Kubota T, Shinohara Y (2018) Comparison of GIS-based landslide susceptibility models using frequency ratio, logistic regression, and artificial neural network in a tertiary region of Ambon, Indonesia. Geomorphology 318:101–111. https://doi.org/10.1016/j.geomorph.2018.06.006

Akgün A, Türk N (2011) Mapping erosion susceptibility by a multivariate statistical method: a case study from the Ayvalık region, NW Turkey. Comput Geosci 37(9):1515–1524

Central Bureau of Statistics of Kulon Progo (2021). https://kulonprogokab.bps.go.id/publication.html

Central Bureau of Statistics of Magelang (2021). https://magelangkab.bps.go.id/publication.html

Central Bureau of Statistics of Purworejo (2021). https://purworejokab.bps.go.id/publication.html

Conforti M, Ietto F (2020) Influence of tectonics and morphometric features on the landslide distribution: a case study from the Mesima Basin (Calabria, South Italy). J Earth Sci 31(2):393–409. https://doi.org/10.1007/s12583-019-1231-z

Erzagian E, Wilopo W, Fathani TF (2023) Landslide susceptibility mapping using frequency ratio method in Kulon Progo Mountains area, Indonesia. AIP Conference Proceedings 2598:070004. https://doi.org/10.1063/5.0127478

Fookes PG, Lee EM, Milligan GC, Press CRC (2005) Geomorphology for engineers: Scotland. Whittles Publishing, Dunbeath, pp 329–337

Geospatial Information Agency of Indonesia (2015-2019) Indonesia's digital topographic map. Bogor, West Java. http://tanahair.indonesia.go.id/portal-web/

Geospatial Information Agency of Indonesia (2023) DEMNAS. https://tanahair.indonesia.go.id/demnas/

Haque U, Da Silva PF, Devoli G, Pilz J, Zhao B, Khaloua A, Glass GE (2019) The human cost of global warming: deadly landslides and their triggers (1995–2014). Sci Total Environ 682:673–684. https://doi.org/10.1016/j.scitotenv.2019.03.415

Ilia I, Tsangaratos P (2016) Applying weight of evidence method and sensitivity analysis to produce a landslide susceptibility map. Landslides 13:379–397

Lee S, Talib JA (2005) Probabilistic landslide susceptibility and factor effect analysis. Environ Geol 47:982–990. https://doi.org/10.1007/s00254-005-1228-z

Mersha T, Meten M (2020) GIS-based landslide susceptibility mapping and assessment using bivariate statistical methods in Simada area, northwestern Ethiopia. Geoenvironmental Disasters 7(1):1–22. https://doi.org/10.1186/s40677-020-00155-x

North MA (2009) A method for implementing a statistically significant number of data classes in the Jenks algorithm. In: Sixth International Conference on Fuzzy Systems and Knowledge Discovery, vol 2009, Tianjin, China, pp 35–38. https://doi.org/10.1109/FSKD.2009.319

Psomiadis E, Papazachariou A, Soulis KX, Alexiou DS, Charalampopoulos I (2020) Landslide mapping and susceptibility assessment using geospatial analysis and earth observation data. Land 9(5):133

Rahardjo W, Sukandarrumidi, Rosidi HMD (1995) Geological map of the Yogyakarta sheet, Java, scale 1:100,000, Geological Survey of Indonesia, Indonesian Ministry of Energy and Mineral Resources

Rasyid AR, Bhandary NP, Yatabe R (2016) Performance of frequency ratio and logistic regression model in creating GIS based landslides susceptibility map at Lompobattang Mountain. Indonesia Geoenviron Disasters 3:19. https://doi.org/10.1186/s40677-016-0053-x

Sarkar S, Kanungo DP (2004) An integrated approach for landslide susceptibility mapping using remote sensing and GIS. Photogramm Eng Remote Sens 70(5):617–625. https://doi.org/10.14358/PERS.70.5.617

Skilodimou HD, Bathrellos GD, Koskeridou E, Soukis K, Rozos D (2018) Physical and anthropogenic factors related to landslide activity in the northern Peloponnese, Greece. Land 7(3):85. https://doi.org/10.3390/land7030085

Tazik E, Jahantab Z, Bakhtiari M, Rezaei A, Alavipanah SK (2014) Landslide susceptibility mapping by combining the three methods fuzzy logic, frequency ratio and analytical hierarchy process in Dozain basin. The International Archives of Photogrammetry, Remote Sensing and Spatial Information Sciences 40(2):267–272. https://doi.org/10.5194/isprsarchives-XL-2-W3-267-2014

Widagdo A, Pramumijoyo S, Harijoko A (2018a) Morphotectono-volcanic of tertiary volcanic rock in Kulon Progo mountains area, Yogyakarta-Indonesia. In IOP Conf.Series: earth and environmental science (Vol. 212, No. 1, p. 012051): IOP Publishing. https://doi.org/10.1088/1755-1315/212/1/012052

Widagdo A, Pramumijoyo S, Harijoko A, Setiyanto A (2018b) Fault lineaments control on disaster potentials in Kulon Progo Mountains area-Central Java-Indonesia. In MATEC Web of Conferences Vol. 229 No. 03008: EDP Sciences

Yalcin A, Bulut F (2007) Landslide susceptibility mapping using GIS and digital photogrammetric techniques: a case study from Ardesen (NE-Turkey). Nat Hazards 41(1):201–226. https://doi.org/10.1007/s11069-006-9030-0